

Hierarchical Optimal Coordination Framework for Connected and Automated Vehicles in Multiple Intersections [★]

Behdad Chalaki ^a, Andreas A. Malikopoulos ^a

^a*Department of Mechanical Engineering, University of Delaware, 126 Spencer Lab, 130 Academy Street, Newark, DE, 19716, USA*

Abstract

In this paper, we present a decentralized optimal control framework for connected and automated vehicles (CAVs) crossing two interconnected intersections. We develop a hierarchical optimization framework that consists of an upper-level and a low-level problems. In the upper-level, we formulate a scheduling problem the solution of which designates the optimal time of each CAV to cross the intersections. The outcome of the upper-level scheduling problem becomes the input of the low-level problem. In particular, in the low-level, we formulate an optimal control problem the solution of which yields the optimal control input (acceleration/deceleration) of each CAV to exit the intersections at the time specified in the upper-level scheduling problem. We demonstrate the effectiveness of the proposed framework through simulation.

Key words: Connected and automated vehicles, interconnected intersections, optimal control, emerging mobility systems

1 Introduction

1.1 Motivation

Due to the increasing population and travel demand, traffic congestion has become a significant concern in big metropolitan areas. By 2050, it is expected that 66% of the population will reside in urban areas; by 2030, there would be 41 Mega-cities (with more than 10M people or more); see [Cassandras \(2017\)](#). [Schrank et al. \(2015\)](#) reported that in 2014, traffic congestion in urban areas in the US caused drivers to spend 6.9 billion additional hours on the road, burning 3.1 billion extra gallons of fuel. Traffic accidents have also increased dramatically over the last decades. In 2015, 35,092 people died on US roadways. However, 94% of serious motor vehicle crashes are due to human error; see [Singh \(2015\)](#).

1.2 Related Work

One of the promising ways to mitigate congestion is the integration of information and communication technologies with cities. Using *connected and automated vehicles*

(CAVs) is one of the intriguing ways towards transitioning to smart cities; see [Klein and Ben-Elia \(2016\)](#) and [Melo et al. \(2017\)](#). CAVs have been used to improve both safety and efficiency of the transportation network using two approaches. The first approach, which gained momentum in the 1980s and 1990s, uses CAVs to reduce vehicle gaps and form high-density platoons to cut congestion; see [Shladover et al. \(1991\)](#) and [Rajamani et al. \(2000\)](#). The second approach smooths the traffic flow to eliminate stop-and-go driving through optimal coordination through traffic bottlenecks; see [Stern et al. \(2018\)](#). Other efforts have been reported in the literature using deep reinforcement learning for training CAVs to achieve smoother traffic flow in different scenarios; see [Sugiyama et al. \(2008\)](#), [Chalaki et al. \(2019\)](#) and [Jang et al. \(2019\)](#).

Several research efforts have been reported in the literature proposing coordination of CAVs. Most studies have focused on traffic bottlenecks such as merging roadways, urban intersections, and speed reduction zones; see [Lioris et al. \(2017\)](#). In earlier work, a decentralized optimal control framework was established for coordinating online CAVs in different transportation scenarios, e.g., merging roadways, urban intersections, speed reduction zones, and roundabouts. The analytical solution without considering state and control constraints, was presented in [Rios-Torres et al. \(2015\)](#), [Rios-Torres and Malikopoulos \(2017\)](#), and [Ntousakis et al. \(2016\)](#)

[★] This research was supported in part by ARPAE's NEXTCAR program under the award number DE-AR0000796 and by the Delaware Energy Institute (DEI).

Email addresses: bchalaki@udel.edu (Behdad Chalaki), andreas@udel.edu (Andreas A. Malikopoulos).

for coordinating online CAVs at highway on-ramps, in Mahbub et al. at two adjacent intersections, and in Zhao et al. (2018) at roundabouts. The solution of the unconstrained problem was also validated experimentally at University of Delaware’s Scaled Smart City using 10 CAV robotic cars in Stager et al. (2018) for a merging roadway scenario and in Beaver et al. (2019) at a corridor. The solution of the optimal control problem considering state and control constraints was presented in Malikopoulos et al. (2018) at an urban intersection without considering rear-end collision avoidance constraint. The conditions under which the rear-end collision avoidance constraint never becomes active were discussed in Malikopoulos et al. (2019). Rios-Torres and Malikopoulos (2016) did a thorough literature review on the different methods of CAVs in their paper and discussed different remaining challenges and potential paths for future research.

Other research efforts have used scheduling theory for tackling the crossing intersection problem; see Ahn et al. (2014), De Campos et al. (2015), Colombo and Del Vecchio (2015), Ahn and Del Vecchio (2016) and Fayazi and Vahidi (2018). Colombo and Del Vecchio (2015) proposed a least restrictive supervisor for intersection with collision avoidance constraints. Ahn et al. (2014) designed a supervisory controller by imposing a hard constraint on safety and studied its behavior in the presence of manual-driven cars. In a sequel paper, Ahn and Del Vecchio (2016) introduced a supervisory controller for an intersection that overrides human-driven control input in case of a future accident. The authors used job-shop scheduling to solve the problem without considering the rear-end collision avoidance constraint. Fayazi and Vahidi (2018) considered a centralized intersection control server that constantly solves an optimization problem for the coming vehicles and passes the optimal arrival time reducing the stop at at the intersection and improving the safety.

1.3 Contribution of this paper

The contribution of this paper is the development of a hierarchical optimization framework to coordinate CAVs at two interconnected intersections. In the upper-level, we formulate a scheduling problem the solution of which designates the optimal time of each CAV to cross the intersections. In the low-level, we formulate an optimal control problem the solution of which yields the optimal control input (acceleration/deceleration) of each CAV to exit the intersections at the time specified in the upper-level scheduling problem. In earlier work, we provided some preliminary results for the scheduling problem by considering constant speed at the merging zone; see Chalaki and Malikopoulos (2019).

1.4 Organizing this paper

The rest of the paper is structured as follows. In Section 2, we introduce the modeling framework and the formulation of both low-level and upper-level optimization problems, while in Section 3, we present the corresponding solutions. Finally, we provide simulation results in Section 4, and concluding remarks along with a discussion for a future research direction in Section 5.

2 Problem Formulation

We consider two interconnected intersections shown in Fig. 1. A drone stores information about the geometric parameters of the intersections, the paths of the CAVs crossing the intersections, and schedules of CAVs. The intersections have a “control zone” (Fig. 1) inside of which the drone can communicate with the CAVs. The drone does not make any decision and it only acts as a “coordinator” among the CAVs. We define the area where lateral collisions may occur as a “merging zone” (Fig. 1).

2.1 Modeling Framework

Let $N(t) \in \mathbb{N}$ be the number of CAVs inside the control zone at time $t \in \mathbb{R}^+$ and $\mathcal{N}(t) = \{1, \dots, N(t)\}$ be the queue that designates the order that each CAV enters the control zone. If two, or more, CAVs enter the control zone at the same time, the CAV with a shorter path receives lower position in the queue; however, if the length of their path is the same, then their position is chosen arbitrarily. We partition the roads around the intersections into $n \in \mathbb{N}$ zones that belong to the set \mathcal{M} . Let \mathcal{I}_i denotes the path of each CAV. When CAV $i \in \mathcal{N}(t)$ enters the control zone, it creates a tuple of the zones $\mathcal{I}_i := [m_1, \dots, m_n]$, $m_n \in \mathcal{M}$, $n \in \mathbb{N}$, that need to cross. Although the number n of partitions is arbitrary, choosing a big number increases the burden of computation for the scheduling problem, since CAV $i \in \mathcal{N}(t)$ needs to find its entry time to each zone. We consider each road connecting to the merging zone to be a single zone. We also partition each merging zone into four smaller zones (Fig. 2). Without being restrictive in our analysis, the total number of zones in the intersections we consider here is $n = 22$.

Definition 1 For each CAV $i \in \mathcal{N}(t)$, we define a tuple $\mathcal{C}_{i,j}$ of conflict zones with CAV $j \in \mathcal{N}(t)$, $j < i$,

$$\mathcal{C}_{i,j} = [m \mid m \in \mathcal{M}, m \in \mathcal{I}_i \wedge m \in \mathcal{I}_j], \quad (1)$$

where the symbol “ \wedge ” corresponds to the logical “AND.”

In Definition 1, the condition $j < i$ implies that CAV i only considers CAVs that are already within the control

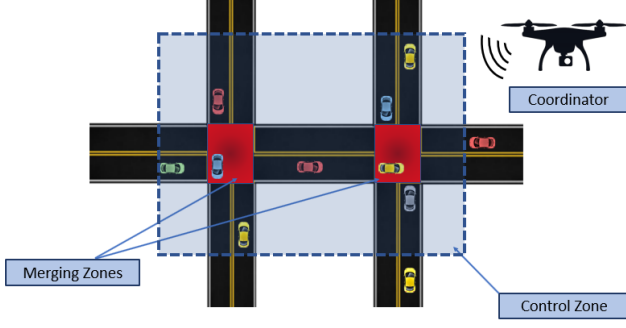


Fig. 1. Two interconnected intersections with a drone as a coordinator.

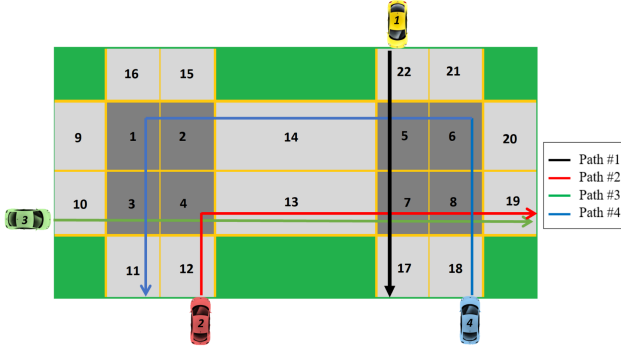


Fig. 2. Zones numbered topologically and the fixed path for each CAV is shown.

zone, i.e., their index in the queue is lower than i . Therefore, CAVs that are already inside the control zone do not need to address potential conflicts with a new CAV entering the control zone. For example in Fig. 2, CAV#3 has the following conflict tuples with CAV#1 and #2 respectively: $\mathcal{C}_{3,1} = [7]$ and $\mathcal{C}_{3,2} = [4, 13, 7, 8, 19]$.

2.2 Vehicle model and assumptions

We model the dynamic of each CAV $i \in \mathcal{N}(t)$ as a double integrator

$$\begin{aligned} \dot{p}_i(t) &= v_i(t), \\ \dot{v}_i(t) &= u_i(t), \end{aligned} \quad (2)$$

where $p_i(t) \in \mathcal{P}_i$, $v_i(t) \in \mathcal{V}_i$, and $u_i(t) \in \mathcal{U}_i$ denote position, speed and acceleration at $t \in \mathbb{R}^+$. Let $\mathbf{x}_i(t) = [p_i(t), v_i(t)]^T$, $u_i(t)$ be the state and control input of the CAV i at time t . Let t_i^0 and t_i^f be the time that CAV $i \in \mathcal{N}(t)$ enters and exits the control zone, and $\mathbf{x}_i^0 = [p_i(t_i^0), v_i(t_i^0)]^T$ be its initial state. For each CAV $i \in \mathcal{N}(t)$ control input and speed is bounded with the following constraints

$$u_{i,min} \leq u_i(t) \leq u_{i,max}, \quad (3)$$

$$0 < v_{min} \leq v_i(t) \leq v_{max}, \quad (4)$$

where $u_{i,min}, u_{i,max}$ are the minimum and maximum control inputs for each CAV $i \in \mathcal{N}(t)$ and v_{min}, v_{max} are the minimum and maximum speed limit respectively. For simplicity, we do not consider diversity among CAVs. Thus, to this end, we set $u_{i,min} = u_{min}$ and $u_{i,max} = u_{max}$. The sets \mathcal{P}_i , \mathcal{V}_i and \mathcal{U}_i , $i \in \mathcal{N}(t)$, are complete and totally bounded subsets of \mathbb{R} .

Definition 2 Let CAV $k \in \mathcal{N}(t)$ be the preceding vehicle of CAV $i \in \mathcal{N}(t)$ in zone $m \in \mathcal{M}$. The distance, $d^m(p_k(t), p_i(t))$, between i and k in zone m is

$$d^m(p_k(t), p_i(t)) = (p_k(t) - d_k^{m,s}) - (p_i(t) - d_i^{m,s}), \quad (5)$$

where $d_i^{m,s}, d_k^{m,s} \in \mathbb{R}^+$ are the distance from the entry point of the control zone to the entry point of the conflict zone m for CAV i and k respectively.

To ensure the absence of rear-end collision between CAV $i \in \mathcal{N}(t)$ and the preceding CAV $k \in \mathcal{N}(t)$ in zone $m \in \mathcal{I}_i \cap \mathcal{I}_k$, we impose the following rear-end safety constraint

$$d^m(p_k(t), p_i(t)) \geq \delta_i(t), \quad (6)$$

where $\delta_i(t)$ is a predefined safe distance. The minimum safe distance $\delta_i(t)$ is a function of speed

$$\delta_i(t) = \gamma_i + \varphi v_i(t), \quad (7)$$

where γ_i is the standstill distance, and φ is the reaction time.

Assumption 1 The path of each CAV is predefined, and all CAVs in the control zone have this information through the drone.

Assumption 2 There is no error or delay in any communication among the CAVs, and the CAVs to the drone.

Assumption 3 The speed at the boundaries of each zone is imposed and known.

Assumption 4 For CAV $i \in \mathcal{N}(t)$ the constraints (4) is not active at entrance of any zone $m \in \mathcal{I}_i$.

The first assumption ensures that when a new CAV enters the control zone, it accesses the memory of the drone and discerns the path of CAVs that are inside the control zone. The second assumption may be strong, but it is relatively straightforward to relax it, as long as the noise or delays are bounded. The third assumption is used to relax the constant speed assumption in the merging zone; see Chalaki and Malikopoulos (2019). We can relax this assumption by estimating the speed at boundaries in the upper-level control for future. The fourth assumption is imposed based on the fact that CAVs would not violate any of the speed limit inside and outside the control zone.

However, we can impose a *feasibility enforcement zone*, preceding the control zone, to ensure that the CAVs enter the control zone with the feasible speed; see Zhang et al. (2017).

2.3 Upper-level Problem: Scheduling

The objective of each CAV inside the control zone is to derive an optimal control input (acceleration/deceleration), which minimizes its travel time and energy consumption. The drone does not make any decision and it only handles information among the CAVs. Each CAV derives its optimal control input in a two-level control framework. In the upper-level control, each CAV uses available information and solves the scheduling problem to compute the appropriate entry time to all zones along its path. Scheduling is a decision-making process that addresses the optimal allocation of resources to tasks over given time periods; see Pinedo (2016). Thus, in what follows, we use scheduling theory to find the time that CAV $i \in \mathcal{N}(t)$ has to reach the zone $m \in \mathcal{I}_i$. Each zone $m \in \mathcal{M}$ represents a “resource,” and CAVs crossing this zone are the “jobs” assigned to the resource.

Definition 3 *The time that a CAV $i \in \mathcal{N}(t)$ enters each zone $m \in \mathcal{I}_i$ is called “schedule” and is denoted by $T_i^m \in \mathbb{R}^+$. For CAV $i \in \mathcal{N}(t)$, we define a “schedule tuple,”*

$$\mathcal{T}_i = [T_i^m \mid m \in \mathcal{I}_i]. \quad (8)$$

For example, the schedule tuple of CAV 1 in Fig. 2 is $\mathcal{T}^1 = [T_1^{22}, T_1^5, T_1^7, T_1^{17}]$.

For each zone $m \in \mathcal{I}_i$, $i \in \mathcal{N}(t)$, the schedule $T_i^m \in \mathbb{R}^+$ is bounded by

$$T_i^{m-1} + R_i^{m-1} \leq T_i^m \leq T_i^{m-1} + D_i^{m-1}, \quad (9)$$

where $R_i^{m-1} \in \mathbb{R}^+$ is the shortest feasible time that it takes for CAV $i \in \mathcal{N}(t)$ to travel through the zone $m-1 \in \mathcal{I}_i$, while $D_i^{m-1} \in \mathbb{R}^+$ is the latest feasible time. Moreover, $R_i^{m-1} \in \mathbb{R}^+$ and $D_i^{m-1} \in \mathbb{R}^+$ are called the *release time* and the *deadline* of the job respectively. The schedule T_i^{m-1} is the time that CAV i enters the zone $m-1$, which is the zone before zone m . The exit time of CAV $i \in \mathcal{N}(t)$ from zone $m \in \mathcal{I}_i$ denoted by $T_i^{m'}$ and is equal to the entry time to zone $m+1 \in \mathcal{I}_i$; zone $m+1$ is the next zone that the CAV crosses right after zone m .

$$T_i^{m'} = T_i^{m+1}. \quad (10)$$

Definition 4 *For CAV $i \in \mathcal{N}(t)$ and $j \in \mathcal{N}(t)$, $j < i$ the safety constraint at the entry of zone $m \in \mathcal{C}_{i,j}$, with the minimum time gap $h \in \Gamma$, can be restated as*

$$|T_i^m - T_j^m| \geq h, \quad (11)$$

where Γ is set of all feasible time which do not activate (6) at the entry of zone m .

Remark 1 *Definition 4 relaxes the first-in-first-out (FIFO) entering policy to the conflict zone by restricting the absolute value of the difference between the two schedules.*

Problem 1 *For each CAV $i \in \mathcal{N}(t)$ with schedule tuple \mathcal{T}_i and minimum time gap $h \in \mathbb{R}^+$, the scheduling problem is formulated as follows*

$$\begin{aligned} \min_{\mathcal{T}_i} \quad & J_i^{[1]}(\mathcal{T}_i) = t_i^f, \\ \text{subject to:} \quad & (9), (11). \end{aligned} \quad (12)$$

In our decentralized scheduling framework, upon entering the control zone, the CAVs solve the scheduling problem sequentially, based on their order at $\mathcal{N}(t)$. Then, they share their schedule tuples with the drone. For example for CAV #3 with $\mathcal{I}_3 = [10, 3, 4, 13, 7, 8, 19]$, $\mathcal{C}_{3,1} = [7]$ and $\mathcal{C}_{3,2} = [4, 13, 7, 8, 19]$, we have the constraint (9) for each zone $m \in \mathcal{I}_3$ as

$$t_3^0 + R_3^{10} \leq T_3^3 \leq t_3^0 + D_3^{10}, \quad (13)$$

$$T_3^3 + R_3^3 \leq T_3^4 \leq T_3^3 + D_3^3, \quad (14)$$

$$T_3^4 + R_3^4 \leq T_3^{13} \leq T_3^4 + D_3^4, \quad (15)$$

$$T_3^{13} + R_3^{13} \leq T_3^7 \leq T_3^{13} + D_3^{13}, \quad (16)$$

$$T_3^7 + R_3^7 \leq T_3^8 \leq T_3^7 + D_3^7, \quad (17)$$

$$T_3^8 + R_3^8 \leq T_3^{19} \leq T_3^8 + D_3^8, \quad (18)$$

$$T_3^{19} + R_3^{19} \leq t_3^f \leq T_3^{19} + D_3^{19}, \quad (19)$$

and from the safety constraint (11) for $m \in \mathcal{C}_{3,1}$ and $m \in \mathcal{C}_{3,2}$ we have

$$|T_3^7 - T_1^7| \geq h, \quad (20)$$

$$|T_3^4 - T_2^4| \geq h, \quad (21)$$

$$|T_3^{13} - T_2^{13}| \geq h, \quad (22)$$

$$|T_3^7 - T_2^7| \geq h, \quad (23)$$

$$|T_3^8 - T_2^8| \geq h, \quad (24)$$

$$|T_3^{19} - T_2^{19}| \geq h, \quad (25)$$

where the schedule tuples of CAV #1 and #2 are accessible through the drone. CAV $i \in \mathcal{N}(t)$ needs to find the release time and the deadline of each zone $m \in \mathcal{I}_i$ prior to solving the scheduling problem (12).

Problem 2 *For each CAV $i \in \mathcal{N}(t)$ and each zone $m \in \mathcal{I}_i$, the release time R_i^m can be found by the following*

optimization problem

$$\begin{aligned} \min_{u_i \in \mathcal{U}_i} \quad & J_i^{[2]}(u_i(t), t) = t_i^{e,m} - t_i^{s,m}, \\ \text{subject to:} \quad & (2), (3), (4), \\ \text{given} \quad & p_i(t_i^{s,m}), v_i(t_i^{s,m}), p_i(t_i^{e,m}), v_i(t_i^{e,m}), \end{aligned} \quad (26)$$

where $t_i^{s,m}$ and $t_i^{e,m}$ are the time that CAV $i \in \mathcal{N}(t)$ enters and exits the zone $m \in \mathcal{I}_i$ respectively. For zone $m \in \mathcal{I}_i$, evaluating the objective function at the optimal $u_i^*(t)$ results in the minimum time that CAV i can travel through zone m which is $R_i^m = t_i^{e,m} - t_i^{s,m}$.

By considering each CAV i to decelerate with $u_i(t) = u_{min}$ and accelerate with $u_i(t) = u_{max}$, each CAV $i \in \mathcal{N}(t)$ can find the deadline D_i^m and release time R_i^m for each zone $m \in \mathcal{I}_i$. If the deadline cannot satisfy either the boundary conditions or the speed constraint, then it decelerates with $u_i(t) = u_{min}$ to reach $v_i(t) = v_{min}$, cruises for some time, and then it accelerates with $u_i(t) = u_{max}$. For example, consider CAV #3. After computing R_3^m and D_3^m for all $m \in \mathcal{I}_3$, it solves the scheduling Problem 1, the solution of which yields the schedule tuple \mathcal{T}^3 .

2.4 Low-level problem: Energy Minimization

After addressing the scheduling in the upper-level problem, in the low-level problem, each CAV derives its minimum control input (acceleration/deceleration) that minimizes the energy consumption; see [Malikopoulos et al. \(2008\)](#). The problem is formulated as follows.

Problem 3 For each CAV $i \in \mathcal{N}(t)$ and each zone $m \in \mathcal{I}_i$, the energy minimization problem is

$$\begin{aligned} \min_{u_i \in \mathcal{U}_i} \quad & J_i^3(u_i(t), T_i^m, T_i^{m'}) = \frac{1}{2} \int_{T_i^m}^{T_i^{m'}} u_i(t)^2 dt, \\ \text{subject to:} \quad & (2), (3), (4), (6), \\ \text{given} \quad & p_i(T_i^m), v_i(T_i^m), p_i(T_i^{m'}), v_i(T_i^{m'}), T_i^m, T_i^{m'}, \end{aligned} \quad (27)$$

where T_i^m and $T_i^{m'}$ are the entry and exit time of CAV $i \in \mathcal{N}(t)$ from zone $m \in \mathcal{I}_i$.

3 Solution of low-level and upper-level problems

In the previous section, we described the hierarchical optimization framework that consists of two upper-level and one low-level problems. Upon entering the control zone, each CAV is added to the queue $\mathcal{N}(t)$, and it solves the upper-level problems (Problems 1 and 2) the solutions of which designate the optimal entry time to

each zone along its path. In the upper-level problems, each CAV first derives the release time and deadline (Problem 2) prior to solving the scheduling problem (Problem 1). The outcome of the upper-level scheduling problem becomes the input of the low-level problem (Problem 3). In particular, in the low-level Problem 3, each CAV derives its optimal control input (acceleration/deceleration) that minimizes energy consumption along its path travelling at the time specified in the upper-level Problem 1. To this end, to simplify notation, we use p_i^s, v_i^s, p_i^e and v_i^e instead of $p_i(t_i^{s,m}), v_i(t_i^{s,m}), p_i(t_i^{e,m})$ and $v_i(t_i^{e,m})$ respectively.

3.1 Analytical solution of the release time and the deadline

For the analytical solution of the release time problem (Problem 2), we apply Hamiltonian analysis. For each CAV $i \in \mathcal{N}(t)$ the Hamiltonian function with the state and control constraints adjoined is

$$\begin{aligned} H_i(t, p_i(t), v_i(t), u_i(t)) = & 1 + \lambda_i^p v_i(t) + \lambda_i^v u_i(t) \\ & + \mu_i^a (u_i(t) - u_{max}) + \mu_i^b (u_{min} - u_i(t)) \\ & + \mu_i^c (v_i(t) - v_{max}) + \mu_i^d (v_{min} - v_i(t)), \end{aligned} \quad (28)$$

where λ_i^p and λ_i^v are costates, and μ^T is a vector of a lagrange multipliers:

$$\mu_i^a = \begin{cases} > 0 & u_i(t) - u_{max} = 0 \\ = 0 & u_i(t) - u_{max} < 0 \end{cases}, \quad (29)$$

$$\mu_i^b = \begin{cases} > 0 & u_{min} - u_i(t) = 0 \\ = 0 & u_{min} - u_i(t) < 0 \end{cases}, \quad (30)$$

$$\mu_i^c = \begin{cases} > 0 & v_i(t) - v_{max} = 0 \\ = 0 & v_i(t) - v_{max} < 0 \end{cases}, \quad (31)$$

$$\mu_i^d = \begin{cases} > 0 & v_{min} - v_i(t) = 0 \\ = 0 & v_{min} - v_i(t) < 0 \end{cases}. \quad (32)$$

The Euler-Lagrange equations become:

$$\dot{\lambda}_i^p = -\frac{\partial H_i}{\partial p_i} = 0, \quad (33)$$

$$\dot{\lambda}_i^v = -\frac{\partial H_i}{\partial v_i} = -\lambda_i^p - \mu_i^c + \mu_i^d. \quad (34)$$

3.1.1 State constraints are not active

First, we consider the case where the state constraint (4) does not become active, hence $\mu_i^c = \mu_i^d = 0$.

Lemma 1 The optimal control input of the release time problem (Problem 2), without the state constraint,

switches at most once, and it can be equal to either $\{u_{min}\}$, or $\{u_{max}\}$, or $\{u_{max}, u_{min}\}$.

Proof: See Appendix A.

Lemma 2 Let $x_i^0 = [p_i^s, v_i^s]^T$ and $x_i^e = [p_i^e, v_i^e]^T$ be the initial and final states of CAV $i \in \mathcal{N}(t)$ travelling in zone $m \in \mathcal{I}_i$. Let $x_i^c = [p_i^c, v_i^c]^T$ be the intermediate state at the switching point. Then,

$$p_i^c = \frac{v_i^{e2} - v_i^{s2} + 2(u_{max}p_i^s - u_{min}p_i^e)}{2(u_{max} - u_{min})}, \quad (35)$$

$$v_i^c = \sqrt{v_i^{s2} + 2u_{max} \cdot (p_i^c - p_i^s)}. \quad (36)$$

Proof. From (2) and Lemma 1, the intermediate states is found by solving the following system of equations

$$\begin{cases} v_i^{c2} - v_i^{s2} = 2u_{max} \cdot (p_i^c - p_i^s) \\ v_i^{e2} - v_i^{c2} = 2u_{min} \cdot (p_i^e - p_i^c) \end{cases}, \quad (37)$$

which yields (35) and (36). \square

Proposition 1 The release time of CAV $i \in \mathcal{N}(t)$ travelling in zone $m \in \mathcal{I}_i$ for the unconstrained case is

$$R_i^m = \frac{v_i^c - v_i^s}{u_{max}} + \frac{v_i^e - v_i^c}{u_{min}}. \quad (38)$$

Proof: The total time is found by integrating (2) for $u_i = u_{max}$ and $u_i = u_{min}$.

$$\begin{aligned} v_i^c - v_i^s &= u_{max} \cdot (t_i^{c,m} - t_i^{s,m}), \quad \forall t \in [t_i^{s,m}, t_i^{c,m}], \\ v_i^e - v_i^c &= u_{min} \cdot (t_i^{e,m} - t_i^{c,m}), \quad \forall t \in [t_i^{c,m}, t_i^{e,m}]. \end{aligned} \quad (39)$$

Solving (39) for $t_i^{c,m}$ and $t_i^{e,m}$, we have

$$t_i^{c,m} = \frac{v_i^c - v_i^s}{u_{max}} + t_i^{s,m}, \quad (40)$$

$$t_i^{e,m} = \frac{v_i^e - v_i^s}{u_{max}} + \frac{v_i^e - v_i^c}{u_{min}} + t_i^{s,m}. \quad (41)$$

Substituting $t_i^{e,m}$ into $R_i^m = t_i^{e,m} - t_i^{s,m}$ we have (38). \square

Proposition 2 Let $x_i^0 = [p_i^s, v_i^s]^T$ and $x_i^e = [p_i^e, v_i^e]^T$ be the initial and final states of CAV $i \in \mathcal{N}(t)$ and $x_i^c = [p_i^c, v_i^c]^T$ be the intermediate state at the switching point. The deadline of CAV i travelling in zone $m \in \mathcal{I}_i$ for the unconstrained case is

$$D_i^m = \frac{v_i^c - v_i^s}{u_{min}} + \frac{v_i^e - v_i^c}{u_{max}}, \quad (42)$$

$$v_i^c = \sqrt{v_i^{s2} + 2u_{min} \cdot (p_i^c - p_i^s)}, \quad (43)$$

$$p_i^c = \frac{v_i^{e2} - v_i^{s2} + 2(u_{min}p_i^s - u_{max}p_i^e)}{2(u_{max} - u_{min})}. \quad (44)$$

Proof: The control input of vehicle $i \in \mathcal{N}(t)$ in zone $m \in \mathcal{I}_i$ consists of two arcs, decelerating with $u_i(t) = u_{min}$ and accelerating with $u_i(t) = u_{max}$. Similarly to the Lemma 2, (44) and (43) are found. The total time for each arc is found by integrating (2)

$$\begin{aligned} v_i^c - v_i^s &= u_{min} \cdot (t_i^{c,m} - t_i^{s,m}), \quad \forall t \in [t_i^{s,m}, t_i^{c,m}], \\ v_i^e - v_i^c &= u_{max} \cdot (t_i^{e,m} - t_i^{c,m}), \quad \forall t \in [t_i^{c,m}, t_i^{e,m}]. \end{aligned} \quad (45)$$

Solving (45) for $t_i^{c,m}$ and $t_i^{e,m}$, we have

$$t_i^{c,m} = \frac{v_i^c - v_i^s}{u_{min}} + t_i^{s,m}, \quad (46)$$

$$t_i^{e,m} = \frac{v_i^c - v_i^s}{u_{min}} + \frac{v_i^e - v_i^c}{u_{max}} + t_i^{s,m}. \quad (47)$$

Substituting $t_i^{e,m}$ into $D_i^m = t_i^{e,m} - t_i^{s,m}$ we have (42). \square

Remark 2 CAV $i \in \mathcal{N}(t)$, travelling in zone $m \in \mathcal{I}_i$ with $D_i^m = t_i^{e,m} - t_i^{s,m}$, activates the state constraint $v_i(t) = v_{min}$, if the speed at the intermediate point derived by (43) is either imaginary, or violates the speed constraint (4).

3.1.2 State constraints are active

Next, We consider the cases where the speed constraints become active.

Theorem 1 In Problem 2, if there is no switching point of the control input, then none of the speed constraints become active.

Proof: We consider the two cases that there is no switching point i.e., Case 1: $\{u_{min}\}$, Case 2: $\{u_{max}\}$.

Case 1: For all $t < t' \in [t_i^{s,m}, t_i^{e,m}]$, we have

$$v_i(t) > v_i(t'), \quad (48)$$

Hence, the minimum and maximum speed can only occur at $t_i^{e,m}$ and $t_i^{s,m}$ respectively, namely

$$\min v_i(t) = v_i^e, \quad \forall t \in [t_i^{s,m}, t_i^{e,m}], \quad (49)$$

and

$$\max v_i(t) = v_i^s, \quad \forall t \in [t_i^{s,m}, t_i^{e,m}]. \quad (50)$$

However, from Assumption 4,

$$v_{min} < v_i^e \leq v_i(t) \leq v_i^s < v_{max}, \quad \forall t \in [t_i^{s,m}, t_i^{e,m}]. \quad (51)$$

Case 2: Similarly to Case 1, we have

$$v_{min} < v_i^s \leq v_i(t) \leq v_i^e < v_{max}, \quad \forall t \in [t_i^{s,m}, t_i^{e,m}]. \quad (52)$$

□

Corollary 1 For CAV $i \in \mathcal{N}(t)$ in zone $m \in \mathcal{I}_i$, the unconstrained solution of the release time problem (Problem 2) can not lead into activating the constrained arc $v_i(t) = v_{min}$.

Proof: From Theorem 1, we consider one switching point, Thus

$$\min v_i(t) = v_i^s, \quad \forall t \in [t_i^{s,m}, t_i^{c,m}], \quad (53)$$

$$\min v_i(t) = v_i^e, \quad \forall t \in [t_i^{c,m}, t_i^{e,m}]. \quad (54)$$

Therefore,

$$\min v_i(t) = v_i^s \text{ or } v_i^e, \quad \forall t \in [t_i^{s,m}, t_i^{e,m}]. \quad (55)$$

From Assumption 4, state constraints are not active at the entry and exit of the zones, and the proof is complete. □

One can check whether the unconstrained solution of CAV i leads to violation of the speed constraint $v_i(t) \leq v_{max}$ in zone m , by checking the speed at the interior point v_i^c found from (36). If the unconstrained solution violates the speed constraint $v_i(t) \leq v_{max}$, then the solution exits the unconstrained arc at time τ_1 , and enters the constrained arc $v_i(t) = v_{max}$. Then the unconstrained arc is pieced together with the constrained arc $v_i(t) = v_{max}$, and we re-solve the problem with the two arcs pieced together. The two arcs yield a set of algebraic equations that are solved simultaneously using the boundary conditions and interior conditions between the arcs. From Assumption 4, the speed at the boundary of zones do not activate the speed constraint; therefore, the solution can not stay at the constrained arc $v_i(t) = v_{max}$ and it must exit the constrained arc $v_i(t) = v_{max}$ at time τ_2 . The unconstrained and constrained arcs are pieced together, and we re-solve the problem with the three arcs pieced together.

Theorem 2 The release time of CAV $i \in \mathcal{N}(t)$ traveling in zone $m \in \mathcal{I}_i$ for the constrained case $v_i(t) = v_{max}$ is

$$R_i^m = \frac{a_i + b_i}{2u_{min} u_{max} v_{max}}, \quad (56)$$

where

$$a_i = v_i^{s^2} u_{min} - v_i^{e^2} u_{max} + (u_{min} - u_{max}) v_{max}^2, \quad (57)$$

$$b_i = 2u_{min} u_{max} (p_i^e - p_i^s) + 2v_{max} (v_i^e u_{max} - v_i^s u_{min}). \quad (58)$$

Proof: See Appendix B.

Proposition 3 Let τ_1 and τ_2 be the time that CAV $i \in \mathcal{N}(t)$ travels in the constrained arc $v_i(t) = v_{min}$, while it is in zone $m \in \mathcal{I}_i$. Let $[p_i^s, v_i^s]^T$ and $[p_i^e, v_i^e]^T$ be the initial and final states of CAV i in zone m respectively. The deadline of CAV i for zone m is computed as follows

$$D_i^m = \frac{v_i^e - v_{min}}{u_{max}} + \tau_2 - t_i^{s,m}, \quad (59)$$

where

$$\tau_2 = \frac{p_i(\tau_2) - p_i(\tau_1)}{v_{min}} + \tau_1, \quad (60)$$

$$p_i(\tau_2) = \frac{v_{min}^2 - v_i^{e^2}}{2 u_{max}} + p_i^e, \quad (61)$$

$$p_i(\tau_1) = \frac{v_{min}^2 - v_i^{s^2}}{2 u_{min}} + p_i^s, \quad (62)$$

$$\tau_1 = \frac{-v_i^s + v_{min}}{u_{min}} + t_i^{s,m}. \quad (63)$$

Proof: See Appendix C.

3.2 Solution of the scheduling problem (Problem 1)

In the scheduling problem (Problem 1), the safety constraint (11) is a disjunctive constraint that

$$T_i^m - T_j^m \geq h, \quad (64)$$

or

$$-(T_i^m - T_j^m) \geq h. \quad (65)$$

In disjunctive constraints, only one constraint has to be satisfied. By introducing a binary variable $B_i \in \{0, 1\}$ and big number $M \in \mathbb{R}^+$, we rewrite the disjunctive constraints as two separate constraints as following:

$$(T_i^m - T_j^m) + B_i \cdot M \geq h, \quad (66)$$

or

$$-(T_i^m - T_j^m) + (1 - B_i) \cdot M \geq h. \quad (67)$$

After transforming the safety constraint to two separate constraints, we use a mixed-integer linear program to solve the scheduling problem. Upon entering the control zone, CAV $i \in \mathcal{N}(t)$ solves the scheduling problem, which results in schedule tuple \mathcal{T}_i .

3.3 Analytical solution of the energy minimization problem (Problem 3)

One approach to address the inequality constraints, which are a function of state variables, is adjoining the q th-order state variable inequality constraint to the Hamiltonian function. The q th-order state variable inequality constraint can be found by taking the successive total time derivative of constraint and substitute (2) for $\dot{\mathbf{x}}$, until we obtain an expression that is explicitly dependent on the control variable; see [Bryson and Ho \(1975\)](#). For each CAV $i \in \mathcal{N}(t)$, with CAV $k \in \mathcal{N}(t)$ positioned immediately in front of it, the Hamiltonian is

$$\begin{aligned} H_i(t, p_i(t), v_i(t), u_i(t)) &= \frac{1}{2}u_i(t)^2 + \lambda_i^p v_i(t) + \lambda_i^v u_i(t) \\ &+ \mu_i^a (u_i(t) - u_{max}) + \mu_i^b (u_{min} - u_i(t)) \\ &+ \mu_i^c (u_i(t)) + \mu_i^d (-u_i(t)) \\ &+ \mu_i^s (v_i(t) - v_k(t) + \varphi u_i(t)). \end{aligned} \quad (68)$$

where λ_i^p and λ_i^v are costates, and μ^T is a vector of a lagrange multipliers.

3.3.1 State and control constraints are not active

If the state and control constraints are not active, $\mu_i^a = \mu_i^b = \mu_i^c = \mu_i^d = 0$ and the solution; see [Malikopoulos et al. \(2018\)](#), is

$$u_i^* = a_i t + b_i, \quad (69)$$

by substituting (69) in (2) we have

$$v_i^* = \frac{1}{2}a_i t^2 + b_i t + c_i, \quad (70)$$

$$p_i^* = \frac{1}{6}a_i t^3 + \frac{1}{2}b_i t^2 + c_i t + d_i. \quad (71)$$

In the above equations a_i, b_i, c_i, d_i are constants of integration, which are found by substituting the initial and final states $p_i(T_i^m), v_i(T_i^m), p_i(T_i^{m'})$ and $v_i(T_i^{m'})$ in zone $m \in \mathcal{I}_i$. Thus, a system of equations in the form of $\mathbf{T}_i \mathbf{b}_i = \mathbf{q}_i$, is

$$\begin{bmatrix} \frac{1}{6}(T_i^m)^3 & \frac{1}{2}(T_i^m)^2 & (T_i^m) & 1 \\ \frac{1}{2}(T_i^m)^2 & (T_i^m) & 1 & 0 \\ \frac{1}{6}(T_i^{m'})^3 & \frac{1}{2}(T_i^{m'})^2 & (T_i^{m'}) & 1 \\ \frac{1}{2}(T_i^{m'})^2 & (T_i^{m'}) & 1 & 0 \end{bmatrix} \cdot \begin{bmatrix} a_i \\ b_i \\ c_i \\ d_i \end{bmatrix} = \begin{bmatrix} p_i(T_i^m) \\ v_i(T_i^m) \\ p_i(T_i^{m'}) \\ v_i(T_i^{m'}) \end{bmatrix}. \quad (72)$$

Note that since (72) can be computed online, the controller may re-evaluate the four constants at any time $t \in [T_i^m, T_i^{m'}]$ and update (69).

There are different cases that can happen and activate either the state or control constraints. Next, we consider the cases that CAV only travels on the constrained arcs except the rear-end safety (6).

3.3.2 CAV travels on different constrained arcs

Case 1: CAV $i \in \mathcal{N}(t)$ enters the constrained arc $u_i(t) = u_{max}$ at T_i^m . Then, it moves to the constrained arc $u_i(t) = u_{min}$ at τ_1 and stays on it until T_i^{m+1} .

Theorem 3 Let T_i^m and T_i^{m+1} be the schedules of CAV $i \in \mathcal{N}(t)$ for zones $m, m+1 \in \mathcal{I}_i$ respectively, where zone $m+1$ follows m . In zone m , the CAV i first travels in the constrained arc $u_i(t) = u_{max}$ and then in the constrained arc $u_i(t) = u_{min}$, if the speed constraint does not become active in zone m and

$$T_i^{m+1} - T_i^m = R_i^m. \quad (73)$$

Proof: Let CAV $i \in \mathcal{N}(t)$ enter and exit the zone $m \in \mathcal{I}_i$ at T_i^m and $T_i^{m'}$ respectively. Substituting (10) into $T_i^{m+1} - T_i^m = R_i^m$, we have $T_i^{m'} - T_i^m = R_i^m$. Thus, CAV i is traveling at earliest feasible time in zone m . Since the speed constraint is not active, the solution is equivalent to the solution of the release time problem (Problem 2) when the speed constraint is not active. \square

In the above case, the optimal control input is

$$u_i^*(t) = \begin{cases} u_{max} & , \text{if } T_i^m \leq t < \tau_1 \\ u_{min} & , \text{if } \tau_1 \leq t \leq T_i^{m'} \end{cases}. \quad (74)$$

Substituting (74) in (2), we have

$$\begin{aligned} p_i^*(t) &= \frac{1}{2}u_{max}t^2 + b_i t + c_i, \\ v_i^*(t) &= u_{max}t + b_i, \quad \forall t \in [T_i^m, \tau_1^-], \end{aligned} \quad (75)$$

$$\begin{aligned} p_i^*(t) &= \frac{1}{2}u_{min}t^2 + d_i t + e_i, \\ v_i^*(t) &= u_{min}t + d_i, \quad \forall t \in [\tau_1^+, T_i^{m'}], \end{aligned} \quad (76)$$

where b_i, c_i, d_i and e_i are constants of integration, which are found by using initial conditions $p_i(T_i^m), v_i(T_i^m)$ and final conditions $p_i(T_i^{m'}), v_i(T_i^{m'})$ of the CAV in zone $m \in \mathcal{I}_i$. The switching point τ_1 can be found from (40).

Case 2: CAV i enters the constrained arc $u_i(t) = u_{max}$ at T_i^m , then it moves to the constrained arc $v_i(t) = v_{max}$ at $t = \tau_1$. It exits the constrained arc $v_i(t) = v_{max}$ at

$t = \tau_2$, and it enters the constrained arc $u_i(t) = u_{min}$ and stays on it until T_i^{m+1} .

Corollary 2 *CAV $i \in \mathcal{N}(t)$ travels in zone $m \in \mathcal{I}_i$ similarly to Case 2, if the speed constraint becomes active in zone m and (73) holds.*

Proof: As in Theorem (3), the solution is equivalent to the solution of the release time problem (Problem 2) when the speed constraint is active. \square

In the above case, the optimal control input is

$$u_i^*(t) = \begin{cases} u_{max} & , \text{if } T_i^m \leq t < \tau_1 \\ 0 & , \text{if } \tau_1 \leq t \leq \tau_2 \\ u_{min} & , \text{if } \tau_2 \leq t \leq T_i^{m'} \end{cases} . \quad (77)$$

Substituting (77) in (2), we have

$$p_i^*(t) = \frac{1}{2}u_{max}t^2 + b_it + c_i, \\ v_i^*(t) = u_{max}t + b_i, \quad \forall t \in [T_i^m, \tau_1^-], \quad (78)$$

$$p_i^*(t) = v_{max} + d_i, \\ v_i^*(t) = v_{max}, \quad \forall t \in [\tau_1^+, \tau_2^-], \quad (79)$$

$$p_i^*(t) = \frac{1}{2}u_{min}t^2 + e_it + f_i, \\ v_i^*(t) = u_{min}t + e_i, \quad \forall t \in [\tau_2^+, T_i^{m'}], \quad (80)$$

where b_i, c_i, d_i, e_i and f_i are constants of integration, and time τ_1 and τ_2 are times that we move from one arc to another arc, which are found by using initial and final conditions in zone m and continuity of states at τ_1 and τ_2 .

Case 3: CAV $i \in \mathcal{N}(t)$ enters the constrained arc $u_i(t) = u_{min}$ at T_i^m . Then, it moves to the constrained arc $u_i(t) = u_{max}$ at τ_1 and stays on it until T_i^{m+1} .

Theorem 4 *Let T_i^m and T_i^{m+1} be the schedules of CAV $i \in \mathcal{N}(t)$ for zones $m, m+1 \in \mathcal{I}_i$ respectively, where zone $m+1$ follows zone m . In zone m , the CAV i first travels in the constrained arc $u_i(t) = u_{min}$ and then at the constrained arc $u_i(t) = u_{max}$, if the speed constraint does not become active in zone m and*

$$T_i^{m+1} - T_i^m = D_i^m. \quad (81)$$

Proof: Let CAV $i \in \mathcal{N}(t)$ enter and exit the zone $m \in \mathcal{I}_i$ at T_i^m and $T_i^{m'}$ respectively. substituting (10) into $T_i^{m+1} - T_i^m = D_i^m$, we have $T_i^{m'} - T_i^m = D_i^m$. Thus, CAV i is traveling at the latest feasible time in zone m . From Proposition (2), CAV i is decelerating with u_{min} and accelerating with u_{max} in zone m . \square

In the latter case, the optimal control input is

$$u_i^*(t) = \begin{cases} u_{min} & , \text{if } T_i^m \leq t < \tau_1 \\ u_{max} & , \text{if } \tau_1 \leq t \leq T_i^{m'} \end{cases} . \quad (82)$$

Substituting (82) in (2), we have

$$p_i^*(t) = \frac{1}{2}u_{min}t^2 + b_it + c_i, \\ v_i^*(t) = u_{max}t + b_i, \quad \forall t \in [T_i^m, \tau_1^-], \quad (83)$$

$$p_i^*(t) = \frac{1}{2}u_{max}t^2 + d_it + e_i, \\ v_i^*(t) = u_{min}t + d_i, \quad \forall t \in [\tau_1^+, T_i^{m'}], \quad (84)$$

where b_i, c_i, d_i and e_i are integration constants, which can be computed by using initial and final conditions of CAV in zone $m \in \mathcal{I}_i$ respectively. The switching point τ_1 can be found from (42).

Case 4: CAV i enters the constrained arc $u_i(t) = u_{min}$ at T_i^m , then it moves to the constrained arc $v_i(t) = v_{min}$ at $t = \tau_1$. It exits the constrained arc $v_i(t) = v_{min}$ at $t = \tau_2$, and it enters the constrained arc $u_i(t) = u_{max}$ and stays on it until T_i^{m+1} .

Corollary 3 *CAV $i \in \mathcal{N}(t)$ travels in zone $m \in \mathcal{I}_i$ as described at Case 4, if the speed constraint becomes active in zone m and (81) holds.*

Proof: As in Theorem (4), CAV i is traveling at the latest feasible time in zone m . From Proposition (3), the proof is complete. \square

In the latter case, the optimal control input is

$$u_i^*(t) = \begin{cases} u_{min} & , \text{if } T_i^m \leq t < \tau_1 \\ 0 & , \text{if } \tau_1 \leq t \leq \tau_2 \\ u_{max} & , \text{if } \tau_2 \leq t \leq T_i^{m'} \end{cases} . \quad (85)$$

Substituting (85) in (2), we have

$$p_i^*(t) = \frac{1}{2}u_{min}t^2 + b_it + c_i, \\ v_i^*(t) = u_{min}t + b_i, \quad \forall t \in [T_i^m, \tau_1^-], \quad (86)$$

$$p_i^*(t) = v_{min} + d_i, \\ v_i^*(t) = v_{min}, \quad \forall t \in [\tau_1^+, \tau_2^-], \quad (87)$$

$$p_i^*(t) = \frac{1}{2}u_{max}t^2 + e_it + f_i, \\ v_i^*(t) = u_{max}t + e_i, \quad \forall t \in [\tau_2^+, T_i^{m'}]. \quad (88)$$

3.3.3 CAV travels on combination of constrained and unconstrained arc

Using (69), we first start with the unconstrained solution of Problem 3. If the solution violates any of the speed (4) or control (3) constraints, then the unconstrained arc is pieced together with the arc corresponding to the violated constraint at unknown time τ_1 , and we re-solve the problem with the two arcs pieced together. The two arcs yield a set of algebraic equations which are solved simultaneously using the boundary conditions and interior conditions at τ_1 . If the resulting solution violates another constraint, then the last two arcs are pieced together with the arc corresponding to the new violated constraint, and we re-solve the problem with the three arcs pieced together at unknown times τ_1 and τ_2 . The three arcs will yield a new set of algebraic equations that need to be solved simultaneously using the boundary conditions and interior conditions at τ_1 and τ_2 . The process is repeated until the solution does not violate any other constraints; see [Malikopoulos et al. \(2018\)](#).

3.3.4 CAV enters the safety constrained arc

Let CAV i enter and exit zone $m \in \mathcal{I}_i$ at T_i^m and $T_i^{m'}$ respectively. CAV k is immediately positioned in front of CAV i in zone m , and CAV i activates the rear-end safety constraint (6) at time $\tau_1 \in [T_i^m, T_i^{m'}]$. We have two cases to consider: Case 1: CAV i remains in the constrained arc until $T_i^{m'}$ or Case 2: CAV i exits the constrained arc at $\tau_2 \in [\tau_1, T_i^{m'}]$.

Lemma 3 *Let CAV i and $k \in \mathcal{N}(t)$ enter the zone m at time T_i^m and T_k^m respectively, and CAV k is immediately ahead of CAV i . CAV i does not activate the rear-end safety constraint at the entry of zone m , if minimum time gap, h , in the upper-level control belongs to the following set*

$$\Gamma = \{t \mid \frac{1}{2}u_{min}t^2 + v_k(T_k^m)t - \varphi v_i(T_i^m) - \gamma_i > 0, \forall t \in \mathbb{R}^+\}. \quad (89)$$

Proof: See Appendix D.

Lemma 4 *If the rear-end safety constraint becomes active for CAV $i \in \mathcal{N}(t)$ at $\tau_1 \in (T_i^m, T_i^{m'})$, then it must exit the rear-end safety constrained arc at $\tau_2 \in [\tau_1, T_i^{m'}]$.*

Proof: From Lemma 3, it follows that CAV i with a schedule $T_i^m \in \mathcal{T}_i$ does not activate the rear-end safety constraint at the entry of zone m for all $m \in \mathcal{I}_i$. Since the exit time of zone m is $T_i^{m'} = T_i^{m+1}$, it does not activate the rear-end safety constraint at the exit of zone m . Thus, if CAV i activates the rear-end safety constraint at τ_1 , it must exit the constrained arc before it exits zone m . \square

3.3.4.1 Hamiltonian analysis when only rear-end safety is active The Hamiltonian (68) when CAV $i \in \mathcal{N}(t)$ enters the rear-end safety constrained arc simplifies to the following.

$$H_i(t, p_i(t), v_i(t), u_i(t)) = \frac{1}{2}u_i(t)^2 + \lambda_i^p v_i(t) + \lambda_i^v u_i(t) + \mu_i^s(t)(S^{(1)}(x_i(t), u_i(t))), \quad (90)$$

where

$$S^{(1)}(x_i(t), u_i(t)) = v_i(t) - v_k(t) + \varphi u_i(t). \quad (91)$$

From the Euler-Lagrange equations we have

$$\lambda_i^p = -\frac{\partial H_i}{\partial p_i} = 0, \quad (92)$$

$$\lambda_i^v = -\frac{\partial H_i}{\partial v_i} = -\lambda_i^p - \mu_i^s, \quad (93)$$

$$\frac{\partial H_i}{\partial u_i} = 0 \text{ or } u_i = -\lambda_i^v - \mu_i^s \varphi. \quad (94)$$

Since the rear-end safety constraint is active, taking the time derivative of (91) we have

$$\dot{u}_i(t) + \frac{1}{\varphi}u_i(t) - \frac{1}{\varphi}u_k(t) = 0. \quad (95)$$

Considering $u_k(t) = a_k t + b_k$ and solving (95) for $u_i(t)$ yields

$$u_i(t) = a_k t + b_k - a_k \varphi + C_1 \exp\left(-\frac{t}{\varphi}\right). \quad (96)$$

Using (96) and solving (92)-(94), we have the following results for λ_i^p , λ_i^v and μ_i^s

$$\lambda_i^p(t) = C_2, \quad (97)$$

$$\mu_i^s(t) = a_k - C_2 - \frac{C_1}{2\varphi} \exp\left(-\frac{t}{\varphi}\right) + C_3 \exp\left(\frac{t}{\varphi}\right), \quad (98)$$

$$\lambda_i^v(t) = C_4 - a_k t - \frac{C_1}{2} \exp\left(-\frac{t}{\varphi}\right) - C_3 \varphi \exp\left(\frac{t}{\varphi}\right). \quad (99)$$

Substituting (96) into (2) we have

$$v_i(t) = \frac{1}{2}a_k t^2 + b_k t - a_k \varphi t - C_1 \varphi \exp\left(-\frac{t}{\varphi}\right) + e_i, \quad (100)$$

$$p_i(t) = \frac{1}{6}a_k t^3 + \frac{1}{2}b_k t^2 - \frac{1}{2}a_k \varphi t^2 + C_1 \varphi^2 \exp\left(-\frac{t}{\varphi}\right) + e_i t + f_i, \quad (101)$$

where e_i , f_i , C_1 , C_2 , C_3 and C_4 are constants of integration.

Theorem 5 Let CAV $i \in \mathcal{N}(t)$ and $k \in \mathcal{N}(t)$ travel in zone m and CAV k is immediately ahead of CAV i . Suppose the control input of CAV k is of the form $u_k(t) = a_k t + b_k$. Then, CAV i does not stay on the rear-end safety constrained arc, and it only activates the rear-end safety constraint instantly, if $a_k \neq 0$ and $b_k \neq 0$.

Proof: See Appendix E.

3.3.4.2 Hamiltonian analysis when only rear-end safety is active for an instant at τ_1 . We have to piece two following unconstrained arcs:

First arc: For all $t \in [T_i^m, \tau_1^-]$

$$u_i(t) = a_i t + b_i, \quad (102)$$

$$v_i(t) = \frac{1}{2} a_i t^2 + b_i t + c_i, \quad (103)$$

$$p_i(t) = \frac{1}{6} a_i t^3 + \frac{1}{2} b_i t^2 + c_i t + d_i. \quad (104)$$

Second arc: For all $t \in [\tau_1^+, T_i^{m'}]$

$$u_i(t) = g_i t + h_i, \quad (105)$$

$$v_i(t) = \frac{1}{2} g_i t^2 + h_i t + m_i, \quad (106)$$

$$p_i(t) = \frac{1}{6} g_i t^3 + \frac{1}{2} h_i t^2 + m_i t + n_i. \quad (107)$$

Since we activate the rear-end safety constraint at $t = \tau_1$, we have an intermediate constraint. Thus, the tangency condition is

$$N(x(\tau_1), \tau_1) = 0, \quad (108)$$

where $N(x(t), t)$ is

$$p_i(t) - p_k(t) + \varphi v_i(t) + \gamma_i + d_k^{m,s} - d_i^{m,s}. \quad (109)$$

We have the following jump conditions:

$$\lambda_i^p(\tau_1^-) = \lambda_i^p(\tau_1^+) + \pi_i \frac{\partial N}{\partial p_i} = \lambda_i^p(\tau_1^+) + \pi_i, \quad (110)$$

$$\lambda_i^v(\tau_1^-) = \lambda_i^v(\tau_1^+) + \pi_i \frac{\partial N}{\partial v_i} = \lambda_i^v(\tau_1^+) + \varphi \pi_i, \quad (111)$$

$$H_i(\tau_1^-) = H_i(\tau_1^+) - \pi_i \frac{\partial N}{\partial t} = H_i(\tau_1^+), \quad (112)$$

$$\frac{\partial H_i}{\partial u_i}(\tau_1^-) = \frac{\partial H_i}{\partial u_i}(\tau_1^+). \quad (113)$$

From the continuity of states of CAV i at τ_1 , we have

$$p_i(\tau_1^-) = p_i(\tau_1^+), \quad (114)$$

$$v_i(\tau_1^-) = v_i(\tau_1^+). \quad (115)$$

$$(116)$$

From the initial and final conditions we have

$$p_i(T_i^m) = p_i^s, \quad (117)$$

$$v_i(T_i^m) = v_i^s, \quad (118)$$

$$p_i(T_i^{m'}) = p_i^e, \quad (119)$$

$$v_i(T_i^{m'}) = v_i^e. \quad (120)$$

We have 10 unknowns for piecing the two unconstrained arcs, which are $a_i, b_i, c_i, d_i, \pi_i, \tau_1, g_i, h_i, m_i, n_i$ and 11 equations, i.e., (108)-(134). However, equation (113) does not give us a useful equation. These equations must be solved simultaneously for piecing two arcs together. If this problem does not have a feasible solution, we must have activated the rear-end safety constraint more than once. However, CAV must still leave the rear-end safety constrained arc immediately after activating it, based on the Theorem 5

4 Simulation results

To evaluate the effectiveness of the proposed framework, we investigate the coordination of 16 vehicles. We consider two symmetrical intersections, where the length of each road connecting to the intersections is 300 m, and the length of the merging zones are 30 m. The minimum time headway is 1 s. The maximum acceleration limit is set to 1 m/s² and the minimum deceleration limit is -1 m/s². The CAVs enter the control zones from four different paths (Fig. 2) at random time with uniform distribution between 0 and 20 s. The desired speed at the boundary is set 20 m/s. Standstill distance and reaction time are set to 5 m and 0.2 s. Upon arriving in the control zone, each CAV solves the upper-level scheduling problem the solution of which designates the optimal time of entry to each zone minimizing the CAV's total travel time.

We present the resulting schedule tuple of each CAV in Table 1. It can be seen from Table 1 that the framework does not limit only one CAV in the merging zones. For example, CAV #2 enters zone 4 at 14.06 s and exit the merging zone at 14.8 s. CAV #3 enters the merging zone at 14.3 s, while CAV #2 is already in the merging zone. Furthermore, CAV #3 enters the zone 4 at 15.06 s and activates the safety constraint (11) at the entry of zone 4 with CAV #2. Moreover, the relative position of CAV #2 and CAV #3 is shown in Fig. 3 for zones which rear-end collision may occur.

The upper-level control provides (11). For instance, CAV #13 and #2 enter the control zone at 13.27 s and 2.05 s respectively. However, CAV #13 enters the zone 7 earlier than CAV #2, CAV #2 should enter the zone 7 earlier than CAV #13, since it arrives earlier to the control zone.

The control input of CAV #15 for its first two zones is shown in Fig. 4. According to Theorem 4, CAV #15

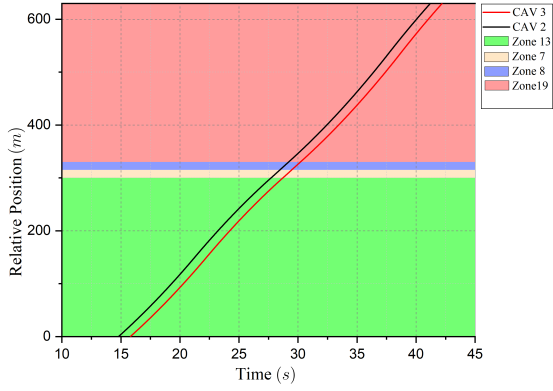


Fig. 3. Relative Position of CAV #2 and CAV #3 in zones which rear-end collision may occur.

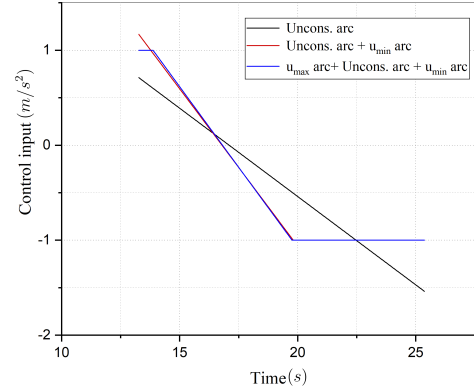


Fig. 5. Control input profile of CAV #13 for zones 22 and 5.

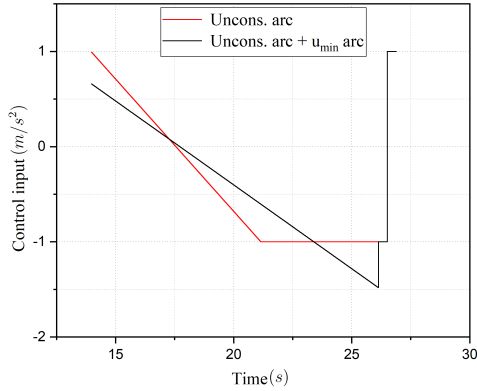


Fig. 4. Control input profile of CAV #15 for zones 10 and 3.

follows u_{min} and then u_{max} trajectory in zone 3. It is shown that the unconstrained trajectory for the zone 10, (shown in black) violates the u_{min} in $t \in [T_{15}^{10}, T_{15}^3]$, thus we pieced unconstrained and corresponding constrained arcs for zone 10, and the resulting trajectory is shown in Fig. 4 (in red).

The control input of CAV #13 for its first zone is shown in Fig. 5. CAV #13 violates the u_{min} in $t \in [T_{13}^{22}, T_{13}^5]$ (shown in black). We pieced unconstrained arc and corresponding constrained arc for zone 22, and the resulting trajectory is shown in Fig. 5 (in red). As it can be seen, the resulting trajectory violates the u_{max} at the beginning. Thus, we pieced constrained arc, u_{max} , the unconstrained arc, and the constrained arc, u_{min} , together. The final trajectory is shown in Fig. 5 (in blue), which does not violate any of the constraints.

The speed for the CAV #13 – #16 is shown in Fig. 6. The relative positions for the CAVs travelling in zone 13 is shown in Fig. 7.

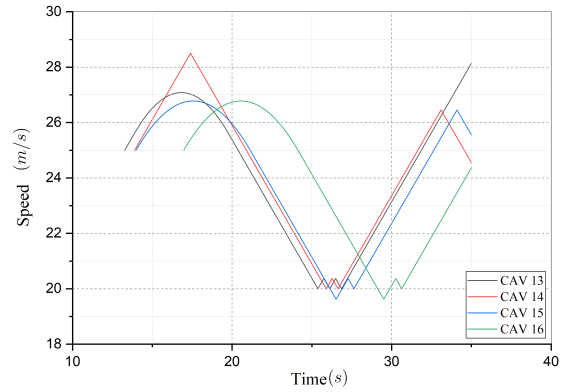


Fig. 6. Speed profile of CAV #13 – #16

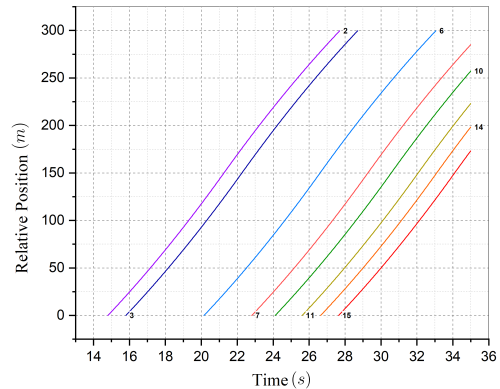


Fig. 7. Relative Position of CAVs travelling in zone 13.

Table 1
Computed Schedules for sixteen CAVs

Path 1										
Index	$t_i^0 = T_i^{22}$	T_i^5	T_i^7	T_i^{17}	t_i^f					
1	0	12.01	12.75	13.49	25.50					
5	5.75	18.80	19.54	20.28	32.29					
9	11.33	23.34	24.08	24.82	36.83					
13	13.27	25.38	26.12	26.86	38.87					
Path 2										
Index	$t_i^0 = T_i^{12}$	T_i^4	T_i^{13}	T_i^7	T_i^8	T_i^{19}	t_i^f			
2	2.05	14.06	14.80	27.72	28.46	29.20	41.21			
6	7.40	19.41	20.15	33.07	33.81	34.55	46.56			
10	11.36	23.37	24.11	37.03	37.77	38.51	50.52			
14	13.89	25.90	26.64	39.56	40.30	41.04	53.05			
Path 3										
Index	$t_i^0 = T_i^{10}$	T_i^3	T_i^4	T_i^{13}	T_i^7	T_i^8	T_i^{19}	t_i^f		
3	2.16	14.30	15.06	15.80	28.72	29.46	30.20	42.21		
7	9.32	21.33	22.07	22.81	35.73	36.47	37.21	49.22		
11	12.12	24.13	24.87	25.61	38.53	39.27	40.01	52.02		
15	13.98	26.14	26.90	27.64	40.56	41.30	42.04	54.05		
Path 4										
Index	$t_i^0 = T_i^{18}$	T_i^8	T_i^6	T_i^5	T_i^{14}	T_i^2	T_i^1	T_i^3	T_i^{11}	t_i^f
4	4.31	16.32	17.06	17.80	18.54	31.46	32.20	32.94	33.68	45.69
8	10.89	22.90	23.64	24.38	25.12	38.04	38.78	39.52	40.26	52.27
12	13.01	25.02	25.76	26.50	27.24	40.16	40.90	41.64	42.38	54.39
16	16.97	30.46	31.20	31.94	32.68	45.60	46.34	47.08	47.82	59.83

5 Concluding Remarks and Future Research

In this paper, we proposed a decentralized optimal control framework for CAVs for two interconnected inter-sections. We established a hierarchical optimal control framework for the coordination of CAVs that consists of two upper-level and on low-level problems. In the upper-level problem, we formulated a scheduling problem that each CAV solves upon entering the control zone. The outcome of the upper-level problem becomes the input of the low-level problem, which is the tuple of proper entry time for each zone to avoid the lateral collision and minimizes the CAV's travel time. In the low-level control, we formulated an optimal control problem the solution of which yields the optimal control input (acceleration/deceleration) minimizes the transient engine operation. We derived an analytical solution for each zone that can be implemented in real time. Finally, we demonstrated the effectiveness of the proposed frame-work through simulation.

There are three potential directions for future research: First, to address uncertainty in data communication and control process in the low-level problem. Second, to investigate the effects of the noise and errors in the upper-level problems. Third, to explore efficient ways of computing the transition time between different arcs, since solving a constrained problem leads to a system of non-linear equations that might be hard to solve in real time.

Appendix A Proof of Lemma 1

If the state constraints for the release time problem (Problem 2) are not active, then $\mu_j^c = \mu_j^d = 0$. Solving (33) and (34) simultaneously yields $\lambda_i^p(t) = a_i$ and $\lambda_i^v(t) = -a_i t + b_i$, where a_i, b_i are the constants of inte-

gration. Hence

$$u_i(t) = \begin{cases} u_{min}, & \text{if } \lambda_i^v(t) > 0 \\ u_{max}, & \text{if } \lambda_i^v(t) < 0 \end{cases}. \quad (121)$$

It follows immediately from the linearity of $\lambda_i^v(t)$ that its sign can change at most once. For the second statement, we use the fact that we can have at most one switching point. There are four cases that we should consider: Case 1: $\{u_{min}\}$, Case 2: $\{u_{max}\}$, Case 3: $\{u_{max}, u_{min}\}$, and Case 4: $\{u_{min}, u_{max}\}$. The initial and final states, denoted by $[p_i^s, v_i^s]^T$ and $[p_i^e, v_i^e]^T$ respectively, are known.

Case 1: If CAV $i \in \mathcal{N}(t)$ decelerates with u_{min} , then from (2) its final speed is

$$v_i^f = \sqrt{2u_{min} \cdot (p_i^e - p_i^s) + v_i^s{}^2}. \quad (122)$$

This case is feasible.

Case 2: If CAV $i \in \mathcal{N}(t)$ accelerates with u_{max} , similarly from (2) its final speed is

$$v_i^f = \sqrt{2u_{max} \cdot (p_i^e - p_i^s) + v_i^s{}^2}. \quad (123)$$

This case is feasible.

Case 3: We have u_{max} then u_{min} , this implies the following:

$$\lambda_i^v(t) = \begin{cases} - , & \text{if } t_i^{s,m} \leq t < t_i^{c,m} \\ 0 , & \text{if } t = t_i^{c,m} \\ + , & \text{if } t_i^{c,m} < t \leq t_i^{e,m} \end{cases}, \quad (124)$$

where $\dot{\lambda}_i^v(t) = -\lambda_i^p(t) = -a_i > 0$. Evaluating the Hamiltonian along the optimal control at time $t_i^{c,m}$ yields

$$H_i(t_i^{c,m}, p_i(t_i^{c,m}), v_i(t_i^{c,m}), u_i(t_i^{c,m})) = 1 + \lambda_i^p v_i(t_i^{c,m}). \quad (125)$$

From the transversality condition,

$$H_i(t_i^{e,m}, p_i(t_i^{e,m}), v_i(t_i^{e,m}), u_i(t_i^{e,m})) = 0. \quad (126)$$

The Hamiltonian (28) must be constant along the optimal solution, since it is not an explicit function of time

$$1 + \lambda_i^p v_i(t_i^{c,m}) = 0. \quad (127)$$

Hence, $v_i(t_i^{c,m}) = -\frac{1}{\lambda_i^p} > 0$. As long as the initial point and endpoint conditions are satisfied, this case is feasible.

Case 4: Similarly to Case 3, it can be shown that $\lambda_i^p(t) = a_i > 0$. Solving (127) for $v_i(t_i^{c,m})$, we have $v_i(t_i^{c,m}) =$

$-\frac{1}{\lambda_i^p} < 0$. Hence, this case cannot be a feasible solution. \square

Appendix B Proof of Theorem 2

Let CAV $i \in \mathcal{N}(t)$ enter and exit the zone $m \in \mathcal{I}_i$ at t_i^s and t_i^e respectively. From the boundary conditions, we have $p_i(t_i^s) = p_i^s, v_i(t_i^s) = v_i^s, p_i(t_i^e) = p_i^e$ and $v_i(t_i^e) = v_i^e$. CAV i cruises with $u_i(t) = u_{max}$, and then it enters the constrained arc $v_i(t) = v_{max}$ at time τ_1 . It stays at the constrained arc with $u_i(t) = 0$ until time τ_2 . After exiting the constrained arc, it decelerates with $u_i(t) = u_{min}$. Substituting optimal control input in (2) results to the following optimal state equations.

$$p_i^*(t) = \frac{1}{2}u_{max}(t^2 - t_i^s{}^2) - u_{max}t_i^s(t - t_i^s) + v_i^s(t - t_i^s) + p_i^s, \\ v_i^*(t) = u_{max}(t - t_i^s) + v_i^s, \quad \forall t \in [t_i^s, \tau_1^-]. \quad (128)$$

$$p_i^*(t) = v_{max}(t - \tau_1) + p_i^*(\tau_1^+), \\ v_i^*(t) = v_{max}, \quad \forall t \in [\tau_1^+, \tau_2^-]. \quad (129)$$

$$p_i^*(t) = \frac{1}{2}u_{min}(t^2 - \tau_2^2) - u_{min}\tau_2(t - \tau_2) \\ + v_i^*(\tau_2^+)(t - \tau_2) + p_i^*(\tau_2^+), \\ v_i^*(t) = u_{min}(t - \tau_2) + v_i^*(\tau_2^+), \quad \forall t \in [\tau_2^+, t_i^e]. \quad (130)$$

The states of CAV are continuous at τ_1 and τ_2 , thus

$$p_i^*(\tau_1^-) = p_i^*(\tau_1^+), \quad (131)$$

$$v_i^*(\tau_1^-) = v_i^*(\tau_1^+), \quad (132)$$

$$p_i^*(\tau_2^-) = p_i^*(\tau_2^+), \quad (133)$$

$$v_i^*(\tau_2^-) = v_i^*(\tau_2^+). \quad (134)$$

From (131)-(134) and the boundary conditions, piecing the unconstrained and constrained arcs together, we have

$$p_i^*(\tau_1) = \frac{1}{2}u_{max}(\tau_1^2 - t_i^s) - u_{max}t_i^s(\tau_1 - t_i^s) \\ + v_i^s(\tau_1 - t_i^s) + p_i^s, \quad (135)$$

$$\tau_1 = \frac{v_{max} - v_i^s}{u_{max}} + t_i^s, \quad (136)$$

$$p_i^*(\tau_2) = v_{max}(\tau_2 - \tau_1) + p_i^*(\tau_1), \quad (137)$$

$$v_i^*(\tau_2) = v_{max}, \quad (138)$$

$$p_i^e = \frac{1}{2}u_{min}(t_i^e{}^2 - \tau_2^2) - u_{min}\tau_2(t_i^e - \tau_2) \\ + v_i^*(\tau_2)(t_i^e - \tau_2) + p_i^*(\tau_2), \quad (139)$$

$$v_i^e = u_{min}(t_i^e - \tau_2) + v_i^*(\tau_2). \quad (140)$$

Solving the system of equations above results to (56). \square

Appendix C Proof of Proposition 3

Let CAV $i \in \mathcal{N}(t)$ enter and exit the zone $m \in \mathcal{I}_i$ at t_i^s and t_i^e respectively. From the boundary conditions, we

have $p_i(t_i^s) = p_i^s$, $v_i(t_i^s) = v_i^s$, $p_i(t_i^e) = p_i^e$ and $v_i(t_i^e) = v_i^e$. CAV i decelerates with $u_i(t) = u_{min}$ then it enters the constrained arc $v_i(t) = v_{min}$ at time τ_1 . It stays at constrained arc with $u_i(t) = 0$ until the τ_2 . After exiting the constrained arc, it cruises with $u_i(t) = u_{max}$. Substituting optimal control input in (2) results to the following optimal state equations.

$$p_i^*(t) = \frac{1}{2}u_{min}(t^2 - t_i^{s2}) - u_{min}t_i^s(t - t_i^s) + v_i^s(t - t_i^s) + p_i^s, \\ v_i^*(t) = u_{min}(t - t_i^s) + v_i^s, \quad \forall t \in [t_i^s, \tau_1^-]. \quad (141)$$

$$p_i^*(t) = v_{min}(t - \tau_1) + p_i^*(\tau_1^+), \\ v_i^*(t) = v_{min}, \quad \forall t \in [\tau_1^+, \tau_2^-]. \quad (142)$$

$$p_i^*(t) = \frac{1}{2}u_{max}(t^2 - \tau_2^2) - u_{max}\tau_2(t - \tau_2) \\ + v_i^*(\tau_2^+)(t - \tau_2) + p_i^*(\tau_2^+), \\ v_i^*(t) = u_{max}(t - \tau_2) + v_i^*(\tau_2^+), \quad \forall t \in [\tau_2^+, t_i^e]. \quad (143)$$

The states of CAV are continuous at τ_1 and τ_2 , thus

$$p_i^*(\tau_1^-) = p_i^*(\tau_1^+), \quad (144)$$

$$v_i^*(\tau_1^-) = v_i^*(\tau_1^+), \quad (145)$$

$$p_i^*(\tau_2^-) = p_i^*(\tau_2^+), \quad (146)$$

$$v_i^*(\tau_2^-) = v_i^*(\tau_2^+). \quad (147)$$

From (144)-(147) and the boundary conditions, piecing the unconstrained and constrained arcs together, we have

$$p_i^*(\tau_1) = \frac{1}{2}u_{min}(\tau_1^2 - t_i^s) - u_{min}t_i^s(\tau_1 - t_i^s) \\ + v_i^s(\tau_1 - t_i^s) + p_i^s, \quad (148)$$

$$\tau_1 = \frac{v_{min} - v_i^s}{u_{min}} + t_i^s, \quad (149)$$

$$p_i^*(\tau_2) = v_{min}(\tau_2 - \tau_1) + p_i^*(\tau_1), \quad (150)$$

$$v_i^*(\tau_2) = v_{min}, \quad (151)$$

$$p_i^e = \frac{1}{2}u_{max}(t_i^e2 - \tau_2^2) - u_{max}\tau_2(t_i^e - \tau_2), \\ + v_i^*(\tau_2)(t_i^e - \tau_2) + p_i^*(\tau_2), \quad (152)$$

$$v_i^e = u_{max}(t_i^e - \tau_2) + v_i^*(\tau_2). \quad (153)$$

Solving the system of equations above results to (59). \square

Appendix D Proof of Lemma 3

Let CAV $i \in \mathcal{N}(t)$ and $k \in \mathcal{N}(t)$ enter the zone m at T_i^m and T_k^m respectively, and CAV k is located in front of CAV i . Since CAV i and k are in the same lane and CAV k is in front, (11) simplifies to $T_i^m \geq T_k^m + h$. For CAV k we have

$$p_k(t) < p_k(t'), \quad \forall t < t' \in \mathbb{R}^+, \quad (154)$$

$$\inf(p_k(T_i^m)) = p_k(T_k^m + h), \quad T_i^m \geq T_k^m + h. \quad (155)$$

Evaluating the (6) at time T_i^m yields

$$(p_k(T_i^m) - d_k^{m,s}) - (p_i(T_i^m) - d_i^{m,s}) \geq \gamma_i + \varphi v_i(T_i^m). \quad (156)$$

Substituting $p_i(T_i^m) = d_i^{m,s}$ and $p_k(T_k^m) = d_k^{m,s}$ into (156) we have

$$(p_k(T_i^m) - p_k(T_k^m)) \geq \gamma_i + \varphi v_i(T_i^m), \quad (157)$$

$(p_k(T_i^m) - p_k(T_k^m)) \geq \inf((p_k(T_i^m) - p_k(T_k^m)))$, (158) where

$$\inf((p_k(T_i^m) - p_k(T_k^m))) = p_k(T_k^m + h) - p_k(T_k^m). \quad (159)$$

If

$$p_k(T_k^m + h) - p_k(T_k^m) > \gamma_i + \varphi v_i(T_i^m) \quad (160)$$

holds, then (157) also holds, and the rear-end safety constraint never becomes active at $t = T_i^m$.

The LHS of (160) corresponds to the distance that CAV k travelled after h seconds from its entry in the zone m , denoted by $\Delta_k^m(h, u_i(t))$. Thus,

$$\operatorname{argmin}_{u_i(t)} \Delta_k^m(h, u_i(t)) = u_{min}. \quad (161)$$

Substituting (161) and $t = h$ into (2), we have

$$\Delta_k^m = \frac{1}{2}u_{min}h^2 + v_i(T_k^m)h \quad (162)$$

If (162) is greater than $\gamma_i + \varphi v_i(T_i^m)$, it yields (160), and the proof is complete.

Appendix E Proof of Theorem 5

CAV $i \in \mathcal{N}(t)$ enters the constrained arc at $t = \tau_1$ from unconstrained energy-optimal arc and exit the constrained arc at $t = \tau_2$ to the unconstrained arc again. We have to piece together the following arcs:

First arc: For $t \in [T_i^m, \tau_1^-]$

$$u_i(t) = a_i t + b_i, \quad (163)$$

$$v_i(t) = \frac{1}{2}a_i t^2 + b_i t + c_i, \quad (164)$$

$$p_i(t) = \frac{1}{6}a_i t^3 + \frac{1}{2}b_i t^2 + c_i t + d_i. \quad (165)$$

Second arc: For $t \in [\tau_1^+, \tau_2^-]$

Equations (96),(100) and (101) form the second arc in which the rear-end safety constraint is active.

Third arc: For $t \in [\tau_2^+, T_i^{m'}]$

$$u_i(t) = g_i t + h_i, \quad (166)$$

$$v_i(t) = \frac{1}{2} g_i t^2 + h_i t + m_i, \quad (167)$$

$$p_i(t) = \frac{1}{6} g_i t^3 + \frac{1}{2} h_i t^2 + m_i t + n_i. \quad (168)$$

At the entry to the constraint arc, we have the following tangency and jump conditions

$$N(x(t), t) = p_i(t) - p_k(t) + \varphi v_i(t) + \gamma_i = 0, \quad (169)$$

$$\lambda_i^p(\tau_1^-) = \lambda_i^p(\tau_1^+) + \pi_i \frac{\partial N}{\partial p_i} = \lambda_i^p(\tau_1^+) + \pi_i, \quad (170)$$

$$\lambda_i^v(\tau_1^-) = \lambda_i^v(\tau_1^+) + \pi_i \frac{\partial N}{\partial v_i} = \lambda_i^v(\tau_1^+) + \varphi \pi_i, \quad (171)$$

$$H_i(\tau_1^-) = H_i(\tau_1^+) - \pi_i \frac{\partial N}{\partial t} = H_i(\tau_1^+), \quad (172)$$

$$\frac{\partial H_i}{\partial u_i}(\tau_1^-) = \frac{\partial H_i}{\partial u_i}(\tau_1^+). \quad (173)$$

The π_i is the constant of lagrange multiplier where determined to satisfy the condition (169), which is found from :

$$[\pi_i \left[\frac{\partial N}{\partial p_i} \frac{\partial N}{\partial v_i} \right] \begin{bmatrix} v_i(t) \\ u_i(t) \end{bmatrix} + \frac{1}{2} u_i^2(t)]_{t=\tau_1} = 0. \quad (174)$$

At the exit point of the constrained arc we have

$$\lambda_i^p(\tau_2^-) = \lambda_i^p(\tau_2^+), \quad (175)$$

$$\lambda_i^v(\tau_2^-) = \lambda_i^v(\tau_2^+), \quad (176)$$

$$H_i(\tau_2^-) = H_i(\tau_2^+), \quad (177)$$

$$\frac{\partial H_i}{\partial u_i}(\tau_2^-) = \frac{\partial H_i}{\partial u_i}(\tau_2^+). \quad (178)$$

Continuity of states of CAV i at τ_1 and τ_2 yield following equations:

$$p_i(\tau_1^-) = p_i(\tau_1^+), \quad (179)$$

$$v_i(\tau_1^-) = v_i(\tau_1^+), \quad (180)$$

$$p_i(\tau_2^-) = p_i(\tau_2^+), \quad (181)$$

$$v_i(\tau_2^-) = v_i(\tau_2^+). \quad (182)$$

The initial and final conditions yield the following equations:

$$p_i(T_i^m) = p_i^s, \quad (183)$$

$$v_i(T_i^m) = v_i^s, \quad (184)$$

$$p_i(T_i^{m'}) = p_i^e, \quad (185)$$

$$v_i(T_i^{m'}) = v_i^e. \quad (186)$$

Since the Hamiltonian does not depend explicitly on time, the Hamiltonian is constant along the optimal trajectory. Therefore, substituting (96),(97) and (99) into

the Hamiltonian of the second arc (90) yields the following:

$$H_i(t) = \frac{1}{2} u_i(t)^2 + \lambda_i^p v_i(t) + \lambda_i^v u_i(t) \quad (187)$$

$$+ \mu_i^s(t) (S^{(1)}(x_i(t), u_i(t))), \quad (188)$$

$$(189)$$

on the rear-end safety constrained arc, we have

$$S^{(1)}(x_i(t), u_i(t)) = 0. \quad (190)$$

$$\begin{aligned} H_i(t) = & C_4 b_k + C_2 e_i + \frac{b_k^2}{2} + \frac{a_k^2 \varphi^2}{2} - \frac{a_k^2 t^2}{2} \\ & + \frac{C_1 b_k e^{-\frac{t}{\varphi}}}{2} - C_1 C_3 \varphi - C_4 a_k \varphi + C_4 a_k t \\ & + C_2 b_k t - a_k b_k \varphi + \frac{C_2 a_k t^2}{2} \\ & + C_1 C_4 e^{-\frac{t}{\varphi}} - C_1 C_2 \varphi e^{-\frac{t}{\varphi}} \\ & - \frac{C_1 a_k \varphi e^{-\frac{t}{\varphi}}}{2} - C_3 b_k \varphi e^{t/\varphi} - \frac{C_1 a_k t e^{-\frac{t}{\varphi}}}{2} \\ & + C_3 a_k \varphi^2 e^{t/\varphi} - C_2 a_k \varphi t - C_3 a_k \varphi t e^{t/\varphi}. \end{aligned} \quad (191)$$

For having (191) to be time-invariant, we have the following:

$$\frac{\partial H_i}{\partial t} = 0. \quad (192)$$

Taking partial derivative of (191) and setting it to zero gives the following equation:

$$\begin{aligned} \frac{\partial H_i}{\partial t} = & C_4 a_k + C_2 b_k - C_2 a_k \varphi \\ & - a_k^2 t + C_2 a_k t \\ & - C_3 b_k e^{t/\varphi} \\ & - C_3 a_k t e^{t/\varphi} \\ & - \frac{C_1 C_4 e^{-\frac{t}{\varphi}}}{\varphi} - \frac{C_1 b_k e^{-\frac{t}{\varphi}}}{2\varphi} + C_1 C_2 e^{-\frac{t}{\varphi}} \\ & + \frac{C_1 a_k t e^{-\frac{t}{\varphi}}}{2\varphi} = 0. \end{aligned} \quad (193)$$

If the $a_k \neq 0$ and $b_k \neq 0$ for the CAV k , the following equations must hold to satisfy (193)

$$C_4 + b_k - a_k \varphi = 0, \quad (194)$$

$$C_3 = C_1 = 0, \quad (195)$$

$$C_2 = a_k. \quad (196)$$

From equation (175), we get $g_i = a_k$ and from equation (176), we get $h_i = -a_k \varphi + b_k$. Substituting g_i and h_i into the (166) yields the $u_i(t) = a_k t + b_k - a_k \varphi$. Using equation (177), gives the $m_i = e_i$. Using (181), we get $n_i = f_i$. From the above conditions, it can be concluded that second and third arcs are exactly the same, and

CAV i stays in the constrained arc until $T_i^{m'}$, which contradicts the Lemma (4). Therefore, CAV i enters the constrained arc, and leaves it immediately.

References

- H. Ahn and D. Del Vecchio. Semi-autonomous Intersection Collision Avoidance through Job-shop Scheduling. *Proceedings of the 19th International Conference on Hybrid Systems: Computation and Control - HSCC '16*, pages 185–194, 2016.
- H. Ahn, A. Colombo, and D. Del Vecchio. Supervisory control for intersection collision avoidance in the presence of uncontrolled vehicles. In *Proceedings of the American Control Conference*, 2014.
- L. E. Beaver, B. Chalaki, A. Mahbub, L. Zhao, R. Zayas, and A. A. Malikopoulos. Demonstration of a time-efficient mobility system using a scaled smart city (to appear). *arXiv preprint arXiv:1903.01632*, 2019.
- A. E. Bryson and Y. C. Ho. *Applied optimal control: optimization, estimation and control*. CRC Press, 1975.
- C. G. Cassandras. Automating mobility in smart cities. *Annual Reviews in Control*, 44:1–8, 2017.
- B. Chalaki and A. A. Malikopoulos. An optimal coordination framework for connected and automated cavs in two interconnected intersections. In *Proceedings of 2019 IEEE Conference on Control Technology and Applications*, pages 888–893, 2019.
- B. Chalaki, L. Beaver, B. Remer, K. Jang, E. Vinitzky, A. Bayen, and A. A. Malikopoulos. Zero-shot autonomous vehicle policy transfer: From simulation to real-world via adversarial learning. *arXiv preprint arXiv:1903.05252*, 2019.
- A. Colombo and D. Del Vecchio. Least restrictive supervisors for intersection collision avoidance: A scheduling approach. *IEEE Transactions on Automatic Control*, 2015.
- G. R. De Campos, F. Della Rossa, and A. Colombo. Optimal and least restrictive supervisory control: Safety verification methods for human-driven vehicles at traffic intersections. *Proceedings of the IEEE Conference on Decision and Control*, pages 1707–1712, 2015.
- S. A. Fayazi and A. Vahidi. Mixed-integer linear programming for optimal scheduling of autonomous vehicle intersection crossing. *IEEE Transactions on Intelligent Vehicles*, 3(3):287–299, 2018.
- K. Jang, E. Vinitzky, B. Chalaki, B. Remer, L. Beaver, A. A. Malikopoulos, and A. Bayen. Simulation to scaled city: zero-shot policy transfer for traffic control via autonomous vehicles. In *Proceedings of the 10th ACM/IEEE International Conference on Cyber-Physical Systems*, pages 291–300. ACM, 2019.
- I. Klein and E. Ben-Elia. Emergence of cooperation in congested road networks using ICT and future and emerging technologies: A game-based review. *Transportation Research Part C: Emerging Technologies*, 72: 10–28, 2016.
- J. Lioris, R. Pedarsani, F. Y. Tascikaraoglu, and P. Varaiya. Platoons of connected vehicles can double throughput in urban roads. *Transportation Research Part C: Emerging Technologies*, 77:292–305, 2017.
- A. Mahbub, L. Zhao, D. Assanis, and A. A. Malikopoulos. Energy-optimal coordination of connected and automated vehicles at multiple intersections. In *Proceedings of 2019 American Control Conference, 2019*, pp. 2664–2669, 2019.
- A. A. Malikopoulos, D. N. Assanis, and P. Y. Papalambros. Optimal engine calibration for individual driving styles. In *SAE Congress*, 2008.
- A. A. Malikopoulos, C. G. Cassandras, and Y. Zhang. A decentralized energy-optimal control framework for connected automated vehicles at signal-free intersections. *Automatica*, 93:244–256, 2018.
- A. A. Malikopoulos, S. Hong, B. B. Park, J. Lee, and S. Ryu. Optimal control for speed harmonization of automated vehicles. *IEEE Transactions on Intelligent Transportation Systems*, 20(7):2405–2417, 2019.
- S. Melo, J. Macedo, and P. Baptista. Guiding cities to pursue a smart mobility paradigm: An example from vehicle routing guidance and its traffic and operational effects. *Research in Transportation Economics*, 65:24–33, 2017.
- I. A. Ntousakis, I. K. Nikolos, and M. Papageorgiou. Optimal vehicle trajectory planning in the context of cooperative merging on highways. *Transportation Research Part C: Emerging Technologies*, 71:464–488, 2016.
- M. L. Pinedo. *Scheduling: theory, algorithms, and systems*. Springer, 2016.
- R. Rajamani, H.-S. Tan, B. K. Law, and W.-B. Zhang. Demonstration of integrated longitudinal and lateral control for the operation of automated vehicles in platoons. *IEEE Transactions on Control Systems Technology*, 8(4):695–708, 2000.
- J. Rios-Torres and A. A. Malikopoulos. A survey on the coordination of connected and automated vehicles at intersections and merging at highway on-ramps. *IEEE Transactions on Intelligent Transportation Systems*, 18(5):1066–1077, 2016.
- J. Rios-Torres and A. A. Malikopoulos. Automated and Cooperative Vehicle Merging at Highway On-Ramps. *IEEE Transactions on Intelligent Transportation Systems*, 18(4):780–789, 2017.
- J. Rios-Torres, A. A. Malikopoulos, and P. Pisu. Online Optimal Control of Connected Vehicles for Efficient Traffic Flow at Merging Roads. In *2015 IEEE 18th International Conference on Intelligent Transportation Systems*, pages 2432–2437, 2015.
- B. Schrank, B. Eisele, T. Lomax, and J. Bak. 2015 Urban Mobility Scorecard. Technical report, Texas A&M Transportation Institute, 2015.
- S. E. Shladover, C. A. Desoer, J. K. Hedrick, M. Tomizuka, J. Walrand, W.-B. Zhang, D. H. McMahon, H. Peng, S. Sheikholeslam, and N. McKeown. Automated vehicle control developments in the PATH program. *IEEE Transactions on Vehicular Technology*, 40(1):114–130, 1991.

- S. Singh. Critical reasons for crashes investigated in the national motor vehicle crash causation survey. Technical report, 2015.
- A. Stager, L. Bhan, A. A. Malikopoulos, and L. Zhao. A scaled smart city for experimental validation of connected and automated vehicles. In *15th IFAC Symposium on Control in Transportation Systems*, pages 130–135, 2018.
- R. E. Stern, S. Cui, M. L. Delle Monache, R. Bhadani, M. Bunting, M. Churchill, N. Hamilton, H. Pohlmann, F. Wu, B. Piccoli, et al. Dissipation of stop-and-go waves via control of autonomous vehicles: Field experiments. *Transportation Research Part C: Emerging Technologies*, 89:205–221, 2018.
- Y. Sugiyama, M. Fukui, M. Kikuchi, K. Hasebe, A. Nakayama, K. Nishinari, S.-i. Tadaki, and S. Yukawa. Traffic jams without bottlenecks—experimental evidence for the physical mechanism of the formation of a jam. *New journal of physics*, 10(3): 033001, 2008.
- Y. Zhang, C. G. Cassandras, and A. A. Malikopoulos. Optimal control of connected automated vehicles at urban traffic intersections: A feasibility enforcement analysis. In *2017 American Control Conference (ACC)*, pages 3548–3553. IEEE, 2017.
- L. Zhao, A. A. Malikopoulos, and J. Rios-Torres. Optimal control of connected and automated vehicles at roundabouts: An investigation in a mixed-traffic environment. In *15th IFAC Symposium on Control in Transportation Systems*, pages 73–78, 2018.